JOURNAL OF CATALYSIS **164,** 467–476 (1996)
ARTICLE NO. 0403

Methylcyclopentane Ring Opening as a Reaction Test for Pt Catalysts Supported on Non-acidic Materials

Walter E. Alvarez* and Daniel E. Resasco†,[1]

*INTEMA, Universidad Nacional de Mar del Plata, Juan B. Justo 4302, (7600) Mar del Plata, Argentina; and †School of Chemical Engineering, University of Oklahoma, Norman, Oklahoma 73019

Received May 24, 1996; revised August 12, 1996; accepted August 12, 1996

Platinum catalysts supported on non-acidic materials have been prepared and characterized by electron microscopy (TEM), temperature programmed reduction (TPR), hydrogen chemisorption, and methylcyclopentane ring opening reaction. The analysis of the product distribution of this reaction has been shown to be a powerful tool in the study of morphological changes in the catalysts resulting from thermal treatments. Two catalyst series, Pt/L zeolites and Pt/Mg(Al)O, have been investigated using this test reaction. By combining TPR and TEM measurements with the analysis of the 3MP/2MP ratio in the products, it was shown that a high temperature calcination treatment on Pt/L zeolites resulted in a migration of the Pt species out of the zeolite channels. Similarly, the analysis of TPR experiments and the MCP-RO selectivity to *n*-hexane over Pt/Mg(Al)O indicated that, during the preparation of the catalysts, a large fraction of Pt species became trapped inside the bulk of the support and came out to the surface only after a cycle of oxidation/reduction at relatively high temperatures.

INTRODUCTION

Methylcyclopentane has been widely used in catalysis as a probe molecule due to the variety of reaction paths that it can take on different catalysts. For example, it can undergo (a) cracking, which yields products with less than six carbons and mainly occurs at high temperatures or in the presence of Brønsted acid sites; (b) ring enlargement (RE), which has cyclohexane and benzene as main products; and (c) ring opening (RO), which produces C_6 isomers. Ring enlargement and ring opening are in competition. This competition has been illustrated by Bai *et al.* (1, 2) who observed that Pd_n clusters supported over a Y zeolite favor the methylcyclopentane-ring opening (MCP-RO), while $[Pd_nH]^+$ adducts catalyze the methylcyclopentane-ring enlargement (MCP-RE). Similar results have been observed on Pt supported over Y zeolite, Pd/H-mordenite and Pt/H-mordenite (3).

[1] To whom correspondence should be addressed. E-mail: resasco@uoknor.edu.

When the support is non-acidic and the reaction is conducted at low temperatures, the only reaction path that operates is the ring opening. The product distribution of this reaction strongly depends on the structure of the catalyst (4) and, therefore, it contains important information about the catalyst. For example, the product distribution is very sensitive to the presence of foreign species on the catalyst surface such as carbonaceous residues (5), less active metals (6), or sulfur (7). Also, if the support is not an inert material (8) it can also cause structural and promotional changes that can be analyzed by changes in the selectivity of the MCP-RO reaction. For example, it is known that the high temperature reduction of metallic clusters over TiO_2 induces a surface migration of reduced species (TiO_x) from the support to the metallic phase (9). This effect results in loss of catalytic activity, chemisorption capacity, and changes in the selectivity for the MCP-RO reaction (10).

It is generally accepted that over Pt supported catalysts the reaction proceeds by two alternative routes. The so-called *selective mechanism* produces 2MP and 3MP while the *unselective mechanism* produces 2MP, 3MP and nHx in the statistical ratio $2MP:3MP:nHx = 40:20:40$ (11). The first mechanism would involve a tetradsorbed intermediate bonded on surface atoms with a high coordination number. In support of this hypothesis, it has been experimentally verified that, on large metallic particles and low Miller index, the principal RO products are 2MP and 3MP. By contrast, the second mechanism would proceed by a five-carbon ring intermediate bonded to a single atom, producing 2MP, 3MP, and nHx as products. This has also been supported by experimental data that show that small particles of Pt and high Miller index planes yield the statistical distribution (11).

A few years ago, in an attempt to demonstrate the existence of collimating effects in Pt/KLTL catalysts (12), we used the MCP-RO reaction as a test and observed that the selectivity to 3MP was significantly higher than on other Pt catalysts of comparable metal particle size. On the basis of the microgeometry of the system, we proposed that this enhanced selectivity was due to a preferred orientation of the incoming MCP molecule inside the pores of the

0021-9517/96 $18.00

L zeolite with its longer axis parallel to the direction of the pores. According to this arrangement, a MCP molecule reaching a metal particle inside a zeolite cage would be preferentially cleaved through one of its ends. This preferential orientation resulted in a 3MP/2MP ratio higher than the statistical value of 0.5. Similarly, the observed 3MP/*n*H*x* ratio was significantly higher than the statistical value of 0.5. This result was also explained in terms of steric constraints. After entering the zeolite pore, the MCP molecule cannot roll over and consequently only half of the molecules approaching the metal particle with their methyl end would have the H atom in the tertiary C pointing in the right direction to produce *n*-hexane (13).

The aim of the present contribution is to show that the analysis of product distribution of the ring opening of methylcyclopentane can be used to identify structural modifications of the catalyst. We have employed this technique to study the effects of calcination and reduction thermal treatments on two series of Pt catalysts supported on nonacidic materials. For the first series the support is L zeolite, and for the second it is aluminum-stabilized magnesium oxide (Mg(Al)O).

EXPERIMENTAL

Table 1 summarizes the preparation conditions for all the catalysts investigated. The Pt/LTL series was prepared using a KL zeolite, series TSZ-500, BET area 292 m^2/gr, kindly provided by Tosoh Co. To prepare the Ba from, the L zeolite was contacted for 60 hr with a 0.5 *M* solution of $Ba(NO_3)$ using a liquid/solid ratio of 60 ml/gr. After that treatment, the solids were dried and calcined in air at 773 K. The addition of Pt to the L zeolites was carried out by the incipient wetness impregnation technique, using 0.78 ml of an aqueous solution of 4×10^{-5} *M* $Pt(NH_3)_4(NO_3)_2$ (from Aldrich) per gram of zeolite. The resulting samples were dried in air and calcined at various temperatures (from 473 to 773 K). Before the activity measurements, they were reduced *in situ* at 623 or 773 K. The atomic absorption analysis indicated that the Pt/KL catalyst contained 0.6 wt% Pt and 12.2 wt% K, while the Pt/BaKL contained 1.05 wt% Pt, 6.0 wt% Ba, and 8.0 wt% K. In order to have a reference material with the majority of Pt deposited outside the channels of the zeolite, we used the following method. We impregnated the L zeolite with H_2PtCl_6 solution, using a volume ten times larger than the zeolite pore volume. After that, it was dried at 383 K and calcined in flow of air at 673 K for 4 hr. We have identified this catalyst as Pt(out)/KL.

For the second series of catalysts, the aluminum stabilized magnesium oxide (Mg(Al)O) support was prepared by coprecipitation of $Al(NO_3)_3$ and $Mg(NO_3)_2$ (Mallinckrodt pa. grade) from an aqueous solution at 333–348 K. The Mg/Al ratio in the solution was kept at 5 : 1 and the total cation concentration was 1 *M*. A KOH-K_2CO_3 solution was prepared to keep a molar ratio of $CO_3^=/Al = 0.5$ while a KOH solution was continuously added to keep a constant pH of 9. The filtrate was washed with bidistilled water and dried overnight at 353 K. The compound thus obtained, as characterized by XRD, was magnesium aluminum hydroxycarbonate ($MgAlCO_3$) with hydrotalcite (HT) structure. The calcination step was conducted at 873 and 973 K. The final molar ratio measured by atomic absorption analysis was Mg/Al = 4.5/1. A sample of MgO obtained by calcination of $MgCO_3$ was used as a reference.

The catalysts containing 0.5 wt% and 1 wt% Pt over Mg(Al)O were prepared by impregnation of the $MgAlCO_3$–HT support calcined at 873 K, using an aqueous solution of 8.5×10^{-5} *M* H_2PtCl_6 (from Aldrich) to incorporate the metallic precursor. The samples were then dried at room temperature and finally in an oven at 383 K. The calcination step was conducted in air flow (200 cc/min) at 873 K for 4 hr. The reduction step was conducted

TABLE 1

Characteristics of the Catalysts Investigated

Catalyst	Pt loading (wt%)	Platinum precursor	Calcination temperature (K)	Reduction temperature (K)	TEM average Pt particle size (nm)	H/Pt
Pt/KL	0.6	$Pt(NH_3)_4^{2+}$	473	773	—	—
Pt/KL	0.6	$Pt(NH_3)_4^{2+}$	573	773	—	—
Pt/KL	0.6	$Pt(NH_3)_4^{2+}$	623	773	—	—
Pt/KL	0.6	$Pt(NH_3)_4^{2+}$	673	623	1.7 and 11	1.36
Pt/KL	0.6	$Pt(NH_3)_4^{2+}$	673	773	1.7 and 9	—
Pt/KL	0.6	$Pt(NH_3)_4^{2+}$	773	623	—	0.47
Pt(out)/KL	1.0	$PtCl_6^=$	673	773	2.4	0.38
Pt/BaKL	1.05	$Pt(NH_3)_4^{2+}$	673	773	1.7 and 13	1.06
Pt/Mg(Al)O	0.5	$PtCl_6^=$	773	773	—	—
Pt/Mg(Al)O	0.5	$PtCl_6^=$	873	773	2.7	0.37
Pt/Mg(Al)O	1.0	$PtCl_6^=$	773	773	—	—
Pt/Mg(Al)O	1.0	$PtCl_6^=$	873	773	2.4	—

in H_2 flow (30–70 cc/min) for 2 hr at different temperatures.

The final catalysts, as well as the catalyst precursors, were characterized by X-ray diffraction (XRD), atomic absorption (AA), transmission electron microscopy (TEM), temperature programmed reduction (TPR), hydrogen chemisorption, and BET surface area. The XRD measurements were conducted at 40 kV and 20 mA, using CuK_α radiation. Since contact with air for prolonged periods could affect some of the samples, all the pretreatments were done just before the analysis, taking precautions to minimize exposure to air. The TEM observations were conducted in a JEOL 100 CX at 100 kV, at a magnification of 100000x after reduction at 623 or 773 K, passivation, and subsequent exposure to air at room temperature. For the TEM analysis, the samples were crushed in an agate mortar, ultrasound-slurried in isopropyl alcohol, and finally deposited on a carbon film over a Cu grid. The AA analysis was done in a spectrophotometer Instrumentation Laboratory model 551. The BET surface area of $MgAlCO_3$–HT sample showed little variation with the temperature of calcination. It was 185.8 m^2/gr for a sample calcined at 673 K, 191.8 m^2/gr after a calcination at 873 K, and 184 m^2/gr for a sample calcined at 973 K.

Volumetric chemisorption of H_2 was conducted in a static Pyrex system on precalcined samples reduced *in situ* under H_2 flow at different temperatures. Prior to adsorption, the samples were first evacuated at 10^{-4} Torr at the reduction temperature and then at 10^{-5} Torr at room temperature. For the TPR experiments, the samples were pretreated *in situ* in flow of air at different temperatures, cooled to 233 K, and then contacted to a 5% H_2/Ar mixture (flow rate 15 cc/min). A heating rate of 11 K/min was finally applied while the H_2 consumption was continuously measured in a thermal conductivity detector.

The catalytic activity measurements were conducted in a microcatalytic pulse reactor, connected to a GC system equipped with FID and with a DC200 packed column from Supelco. Before each run, the samples were calcined in air flow and reduced *in situ* under H_2 flow. Carbon deposition or sulfur poisoning may greatly alter the catalytic behavior of some of these materials (14, 15). However, the use of a pulse reactor minimizes the deactivation because the amount of sulfur injected in each pulse is extremely small. Based on the level of sulfur in the MCP reagent (<50 ppm), the amount injected (250 μl of 6.8% MCP in H_2), and the Pt load in the reactor (about 2.4×10^{-5} g) we can calculate that the atomic ratio of S/Pt in each pulse was about 2×10^{-5}. Even though it has been shown that each S atom has the apparent ability to deactivate 10 Pt atoms (14), the small number of S atoms injected in each pulse let us work essentially free of sulfur poisoning. In fact, in a control experiment we observed no significant deactivation after 60 consecutive pulses.

RESULTS

Pt/L Zeolites

A series of different Pt/L zeolite samples was prepared by varying the calcination temperature in the range 473–773 K. All the samples were characterized by TPR and DR-UV-visible spectroscopy. The TPR profiles significantly varied among the samples calcined at different temperatures. The sample calcined at 473 K exhibited a large H_2 consumption peak at about 553 K that was almost three times as large as those calcined at higher temperatures. The UV-visible spectroscopy analysis indicated that this sample contained a large fraction of undecomposed $Pt(NH_3)_4^{2+}$ precursor that would account for the large consumption signal in the TPR. For the rest of the samples, UV-visible spectroscopy showed that the precursors were totally decomposed after calcination. Reagan *et al.* (16) studied the dependence of the $Pt(NH_3)_4^{+2}$ complex decomposition on calcination temperature and, in agreement with our results, they observed that the minimum temperature necessary for the decomposition of the precursor during the calcination step was 573 K. The H_2 consumption profiles for the Pt/KL samples calcined at 573 K, 673 K, and 773 K are shown in Fig. 1. For these three samples, the apparent valences (av = moles consumed hydrogen/moles total Pt) calculated from the areas under the TPR peaks, varied between 3 and 3.5. These values suggest that Pt^{2+} and Pt^{4+} species were present in the catalysts.

Similar apparent valences have been obtained by Ostgard *et al.* (17) for a 0.5 wt% Pt/KL catalyst prepared by incipient wetness impregnation and precalcined at 673 K. These authors have discussed the several transformations that occur during the thermal treatments of the impregnated L zeolite. These transformations include decomposition of the $(Pt(NH_3)_4(NO_3)_2)$ precursor, autoreduction of the Pt^{+2} by NH_3, reaction between Pt^{+2} ions and H_2O generating PtO particles, and formation of PtO_2 by oxidation

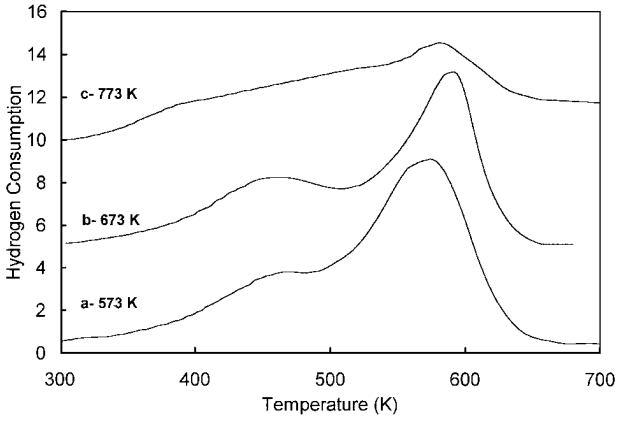

FIG. 1. Temperature programed reduction profiles of $Pt(NH_3)_4^{+2}$/KLTL calcined at different temperatures. (a) 573 K; (b) 673 K; (c) 773 K.

of Pt^{+2} ions or Pt^0 particles. Different amounts of Pt^{2+} and Pt^{4+} species can be present on the catalyst, depending on the thermal treatment and preparation conditions. For example, they observed that for the Pt/KL catalysts prepared by incipient wetness impregnation, the predominant species was Pt^{4+} and, after reduction, the metal particles were predominantly inside the zeolite channels. By contrast, the ion exchange method resulted in a larger fraction of Pt^{2+} species in the calcined sample and, after reduction, a larger fraction of Pt particles outside the zeolite.

For our Pt/KL catalysts, the TPR profiles showed two main peaks at around 480 and 600 K. The size of the high temperature peak clearly decreased when the calcination temperature increased, while the low temperature peak seemed to shift to lower reduction temperatures with increasing calcination temperature. We will discuss the implications of these changes in the next section.

The TEM studies indicated that the Pt/KL zeolite catalysts had a bimodal distribution of Pt particles. Most of the particles were small and located inside the zeolite channels and a few larger particles were located outside the channels. For example, for the sample calcined at 673 K and reduced at 773 K, the average size of the small particles was 1.6 nm while that of the large particles was 9.1 nm. As indicated previously by McVicker *et al.* (14), the particles that appear as large as 1.6 or 1.7 nm, are indeed inside the zeolite channels even though one should not expect them to be larger than the channel size, which is 1.3 nm. The explanation given by these authors is that the width of the electron beam is about 0.4 nm, and, as a result, particles that fit exactly inside the channels may appear as large as 1.7 nm.

The reduction temperature seemed to have a very small effect on the size and location of the metal particles in the zeolite. Samples reduced at different temperatures did not show significant changes in size. On the other hand, the calcination temperature proved to be critical. Similar results have been reported in previous studies by Larsen (18). H/Pt and CO/Pt chemisorption values did not change much with calcination temperatures between 573 and 623 K, but they abruptly decreased at calcination temperatures higher than about 673 K. In agreement with our TEM data, they observed that the reduction temperature had only a minor effect.

We have also used TEM to study the effects of exchanging K^+ by Ba^{2+} cations in the zeolite. The Pt particle size distribution of a Pt/BaL sample was compared to that of a Pt/KL sample treated under identical conditions, i.e., calcination at 673 K and reduction at 773 K. Similar to those supported on KL zeolite, the Pt/BaL catalyst evidenced the presence of a bimodal distribution, with small particles averaging a size of 1.6 nm and large particles averaging 12.7 nm. The size distribution for the small particles (not shown) did not change much when K^+ was exchanged by Ba^{2+}, but that of the larger particles (see Fig. 2) significantly shifted to larger particles.

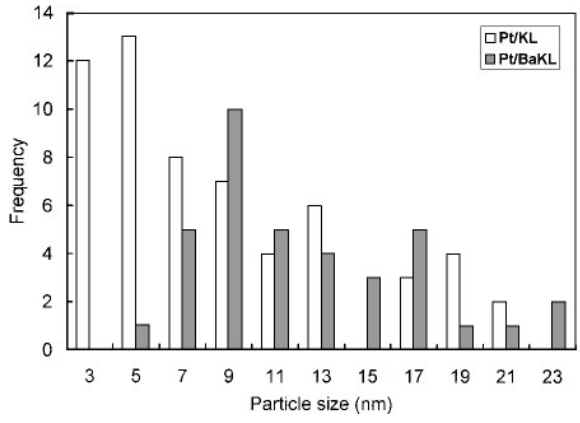

FIG. 2. Size distribution of the larger particles observed by TEM on Pt/KL (open bars) and Pt/BaKL (cross-hatched bars). Both samples were calcined at 673 K and reduced at 773 K.

To further study the structural changes occurring on these catalysts at different calcination temperatures we have analyzed the product distribution of the MCP-RO reaction. The catalytic activity data for the Pt/L samples is summarized in Table 2. As the calcination temperature increased, a decrease was observed in the MCP conversions. The drop in conversion was particularly severe when the calcination temperature increased from 673 to 773 K. However, this decay is not so pronounced when the rates are normalized to the hydrogen chemisorption values and expressed as turnover number. On the other hand, large changes were observed in the distribution of products when compared to the samples calcined at 673 and 773 K. These changes are illustrated in Fig. 3 which shows the variation of the chemisorption capacity, H/Pt, together with the variation of the 3MP/2MP ratio as a function of the calcination temperature. A remarkable correlation can be observed between the decrease in chemisorption capacity (H/Pt) and the 3MP/2MP ratio in the products.

Table 2 also includes data obtained over the Pt/BaL catalyst. One can compare the MCP-RO activity of this catalyst to that of the Pt/KL treated under the same conditions. The rate per gram of Pt for the Pt/BaL catalyst is more than three times lower than that for the Pt/KL catalyst. However, this activity difference is not paralleled by a similar difference in hydrogen chemisorption capacity. At the same time, the 3MP/2MP product ratio is much lower for the Pt/BaL than for the Pt/KL. As we will discuss below, we attribute these differences to a partial blocking of the zeolite channels by Ba^{2+} cations which would not occur on the KL zeolite treated under the same conditions.

Pt/Mg(Al)O Catalysts

The Al-stabilized magnesium oxide (Mg(Al)O) is an interesting system to compare to the L zeolites because it

TABLE 2

Catalytic Activity and Selectivity of Pt/LTL and Pt/Mg(Al)O Catalysts for the MCP-RO Reaction

Catalyst	Platinum loading (wt%)	Calcination temperature (K)	Reduction temperature (K)	Reaction temperature (K)	H/Pt ratio	Conversion (%)	TON (sec^{-1})	3MP/2MP ratio
0.6% Pt/KL	0.6	473	623	613	—	20.1	—	0.89
0.6% Pt/KL	0.6	573	623	613	—	13.5	—	0.90
0.6% Pt/KL	0.6	623	623	613	—	6.1	—	0.86
0.6% Pt/KL	0.6	673	623	613	1.36	7.5	0.21	0.84
0.6% Pt/KL	0.6	773	623	613	0.47	2.2	0.18	0.62
1% Pt/BaKL	1.0	673	773	613	1.06	3.9	0.084	0.39
0.6% Pt/KL	0.6	673	623	603	1.36	4.8	0.14	0.89
0.6% Pt/KL	0.6	773	623	603	0.47	1.3	0.11	0.58
1% Ptout/KL	1.0	673	773	603	0.385	6.6	0.4	0.32
Pt/Mg(Al)O	0.5	873	773	603	0.373	1.76	0.16	0.28
Pt/Mg(Al)O	0.5	773	773	603	—	8.9	—	0.26

does not exhibit the microporosity of the zeolites (19), but yet it promotes the aromatization activity. This material can be synthesized from magnesium aluminum hydroxycarbonate ($MgAlCO_3$) with hydrotalcite (HT) structure. The $MgAlCO_3$–HT has a brucite structure in which some M^{+2} cations are replaced by M^{+3} cations in the framework, in this case, Mg^{2+} are replaced by Al^{3+}. As a result, the structure presents an excess charge due to the presence of M^{3+} cations. This excess charge is compensated by anions, such as CO_3^{2-}, intercalated in the brucite layers (20, 21). After calcination, this compound has a high surface area, basic properties, and thermal stability.

We have synthesized and characterized this material during several stages in the synthesis process. Figure 4 shows the XRD spectra for $MgAlCO_3$–HT, a MgO reference, and the Mg(Al)O support obtained from the calcination of the $MgAlCO_3$–HT at 873 K. From the XRD patterns it is clear that the Mg(Al)O exhibits the same structure as the MgO. As illustrated in Fig. 5, a total reconversion to the hydrotalcite structure was obtained when the Mg(Al)O support was impregnated with the H_2PtCl_6 solution during the preparation of the catalyst. The typical MgAl–HT XRD profile was observed on the impregnated sample, but this structure disappeared again when the catalyst was calcined at 873 K. This "memory effect" has been previously observed by other authors. After losing the hydrotalcite structure by calcination, the material can rebuild its original structure when it is contacted with aqueous solutions containing $CO_3^{=}$ anions (22, 23). We report here that the same effect occurs when the calcined material is contacted with H_2PtCl_6 (or even HNO_3) solutions.

After calcination and reduction in H_2 at 773 K, the H/Pt chemisorption values of the resulting Pt/Mg(Al)O catalysts, varied between 0.31 and 0.37, while the average Pt particle size, as determined by TEM, was 2.4–2.7 nm.

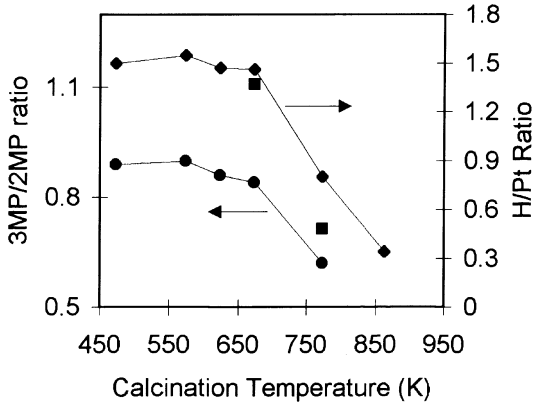

FIG. 3. 3-methylpentane/2-methylpentane product ratio (left axis) and H/Pt chemisorption capacities (right axis) as a function of calcination temperature on the 0.6% Pt/KLTL catalyst. (●) 3MP/2MP ratio; (◆) H/Pt, from Ref. 18; (■) H/Pt, this work. Reduction temperature: 623 K. MCP-RO reaction temperature: 613 K.

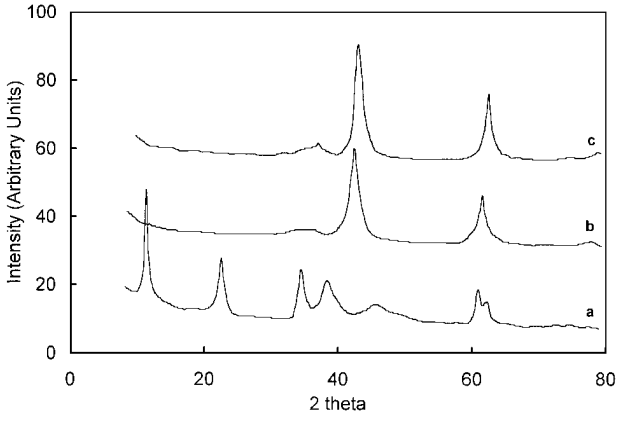

FIG. 4. X-ray diffraction patterns: (a) hydrotalcite structure of $MgAlCO_3$–HT, with a Mg/Al ratio of 4.5; (b) Mg(Al)O obtained by calcination of $MgAlCO_3$–HT at 873 K; (c) MgO reference obtained by decomposition of $MgCO_3$ at 973 K.

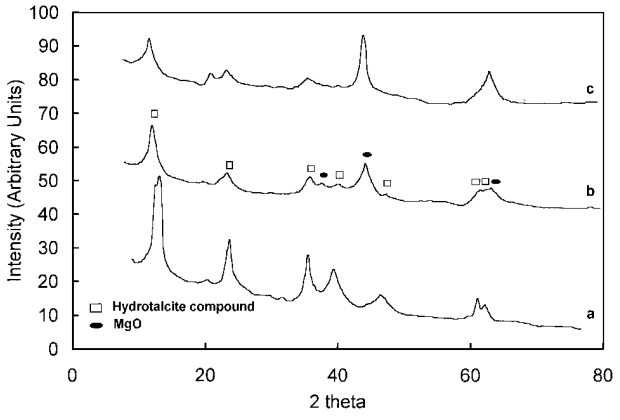

FIG. 5. X-ray diffraction patterns: (a) Mg(Al)O support impregnated with H_2Cl_6Pt solution; (b) sample (a) calcined at 773 K; (c) sample (a) calcined at 873 K. The open squares indicate positions that correspond to hydrotalcite structure, and the ovals indicate positions that correspond to MgO.

The Pt/Mg(Al)O catalysts were also characterized by TPR. Prior to the TPR analysis, the samples were calcined *in situ* at 773 K. Sequential TPR experiments with intermediate calcinations at 773 K were conducted on each sample. For all the samples, including the Mg(Al)O support, the first TPR showed H_2 consumptions starting at 643 K and extending to temperatures above 773 K, while the magnitude of the peaks for the second TPR was much smaller. We believe that this difference in consumption is due to a dehydroxilation of the Mg(Al)O that occurs only during the first TPR.

To focus on the analysis of the Pt species and eliminate the hydrogen consumption due to the support, we report in Fig. 6 the difference TPR for the Pt/Mg(Al)O catalyst. These profiles have been obtained by subtracting the signal obtained on the bare support. Interesting features are observed when the sequential TPR profiles are compared. The first TPR exhibited a H_2 consumption at relatively high temperatures, while the subsequent cycles presented two peaks at much lower temperatures. An increase in consumption was observed in this region for the second cycle but it did not change significantly for the following cycles. A clear change in the state of the catalyst occurs during the first cycle that is not present in the subsequent cycles. From the areas under the peaks, an increase of about 40% in the H_2 consumption was measured during the second and third cycles in comparison to the first one. This increase would suggest that a fraction of Pt was not exposed to the gas phase during the first cycle.

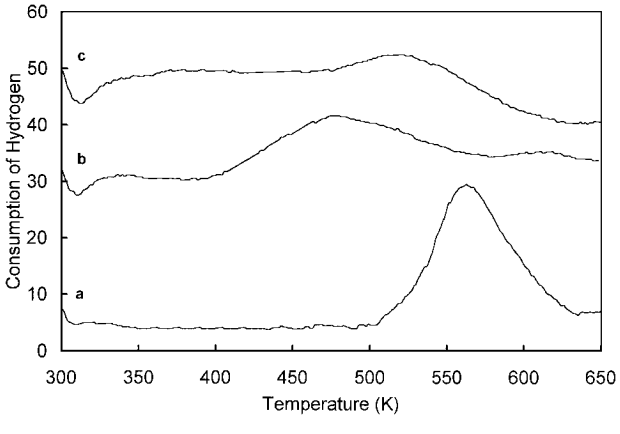

FIG. 6. Sequence of TPR experiments on 1%Pt/Mg(Al)O catalyst: (a) first TPR on a fresh sample calcined in air at 773 K; (b) second TPR, conducted after (a) and calcined at 773 K; (c) third TPR, conducted after (b) and calcined at 773 K.

The MCP-RO activity data obtained on the Pt/Mg(Al)O series are included in Table 2. As shown in the table, we observed that, as opposed to the ratios observed on the Pt/L catalysts, the 3MP/2MP ratios were significantly lower than the statistical value of 0.5.

In parallel to the remarkable differences observed in the TPR experiments between the first oxidation–reduction cycle and the subsequent cycles, a very peculiar behavior was observed in the MCP-RO activity of these catalysts over the sequence of oxidation–reduction cycles. The Pt/Mg(Al)O samples was calcined *in situ* at either 773 or 873 K for 2 hr and then reduced at increasing temperatures. Figure 7 shows the variation of conversion and percent of *n*-Hexane in products as a function of the reduction temperature for the first and second oxidation–reduction cycles. A distinct trend has been observed for all the Pt/Mg(Al)O catalysts investigated. During the first cycle, the overall activity increased when the reduction temperature increased from 623 to 773 K. This increase was accompanied by an increase in the selectivity toward *n*-hexane. By contrast, during the subsequent oxidation–reduction cycle the opposite behavior was obtained; i.e., both the activity and the *n*-hexane selectivity decreased when the reduction temperature increased. The same behavior was observed in the subsequent cycles.

DISCUSSION

During the last several years, Pt catalysts supported on non-acidic materials have received renewed attention as they can be very active and selective for the aromatization of C_6 alkanes. First, it was found that Pt/L zeolites displayed unique catalytic properties for these reactions (24, 25), but more recently it was found that Pt supported over alumina stabilized magnesium oxide (Pt/Mg(Al)O) also presented high aromatization activity and selectivity (26, 27). The fundamental reason behind the unique properties of Pt supported on non-acidic materials is still a matter of discussion. Some authors have proposed that the Pt clusters are modified by a metal–support interaction which favors the production of aromatics (28). The fact that both zeolitic

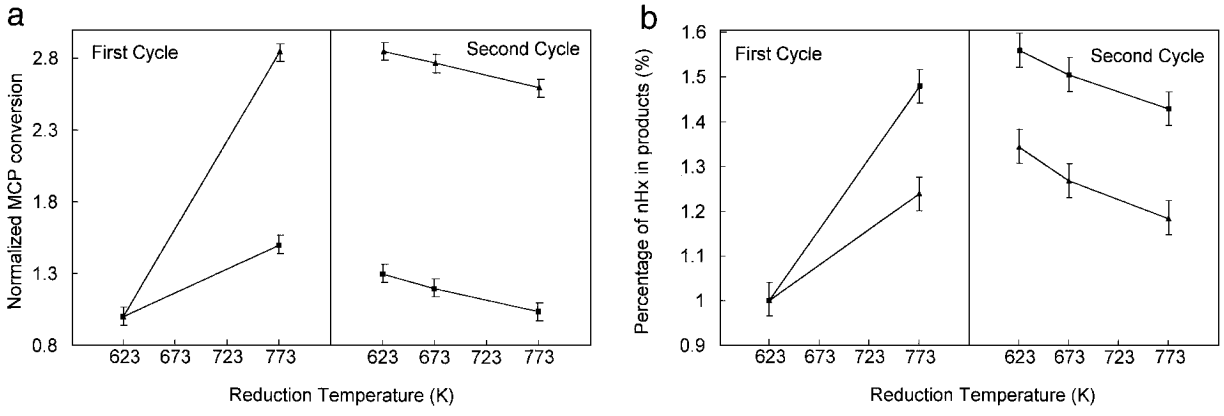

FIG. 7. (a) Catalytic activity and (b) Selectivity to *n*-hexane obtained on 1%Pt/Mg(Al)O catalysts for the MCP-RO as a function of reduction temperature at a reaction temperature of 603 K. Left panels: first reaction cycle. Right panels: second reaction cycle, after first cycle and calcination at 773 K. The activity and selectivity values are normalized to the activity and selectivity values obtained during the first cycle on the catalyst reduced at 623 K. First calcination temperature: 773 K (■) and 873 K (▲).

and non-zeolitic supports exhibit the same promoting effects have lead some to believe that the very small Pt particles have excess negative charge either when they are into the zeolite L channels (29, 30) or when they are deposited on the surface of the Mg(Al)O support (31). A diverging view has been presented based almost entirely on geometric arguments (32), a molecular-die model was proposed to explain the unique ability of Pt/LTL catalysts to aromatize C_6 alkanes. This model, however does not explain the ability of the Mg(Al)O to promote aromatization. More recently, Iglesia and Baumgartner (33) have also considered geometric arguments to explain the high aromatization selectivity of Pt/LTL. However, their descriptions focus more on the shape selective ability of the catalyst to inhibit the formation of coke rather than on a configurational diffusion as implied by the molecular-die model. According to these authors, the high benzene selectivity would be an intrinsic property of clean Pt but it is rapidly lost when Pt is poisoned by carbon deposits. The unique ability of the zeolite LTL would be to inhibit the rate of carbon deposition that would otherwise cause the loss of aromatization activity. The narrow one-dimensional channels of the L zeolite would inhibit the bimolecular reactions that lead to the polymerization of coke precursors. This proposal does not explain that a basic support without microporosity, such as Mg(Al)O, still exhibits high aromatization selectivity (34), while a nonacidic molecular sieve with unidimensional channels such as SSZ-24 fails to promote aromatization (35).

In our previous study (12) of MCP-RO on Pt/KL catalysts, we demonstrated that collimation effects were indeed present for the hydrogenolysis of MCP. We did not study the aromatization reaction although the underlying consequence was that collimation effects could play an important role in other hydrocarbon reactions on Pt/KL catalysts, including *n*-hexane aromatization. The more recent results showing that this reaction can be promoted by Mg(Al)O, which does not have mocroporosity, suggest that collimation effects alone cannot explain the *n*-hexane aromatization activity. What we want to emphasize in this contribution is that collimation effects do play a role in MCP-RO, and this reaction is an excellent tool to characterize supported metal clusters.

For example, we can combine the analysis of MCP-RO reaction with other characterization techniques to describe the effects of calcination on the final structure, and consequently the catalytic properties of the Pt/LTL zeolites. The TPR profiles of the samples calcined at higher temperatures provide an interesting basis for the discussion that will follow about the MCP-RO reaction. As shown in Fig. 6, when the calcination temperature increased to 773 K, the low temperature peak shifted to even lower temperatures while the high temperature peak decreased in magnitude. We interpret these changes in terms of a migration of Pt species generated by the calcination treatment. The high temperature peak can be associated with Pt^{4+} species located inside the zeolite channels and the low temperature peak with Pt^{2+} species located outside the zeolite. The observed changes in TPR profiles would indicate that as the calcination temperature increases, a fraction of Pt species inside the channels of the zeolite are leached out and grow as larger particles outside.

For the Pt/KL catalysts, the increase in calcination temperature caused a gradual decrease in the overall specific MCP-RO reaction rate but not a significant decay in the turnover frequency. This could be interpreted in terms of a simple lost of Pt sites, both for reaction as well as for hydrogen chemisorption, which can be related to Pt particle growth. However, the analysis of the product distribution can provide finer details about the nature of the particle growth process. For example, the 3MP/2MP ratio has been

found on many Pt catalysts to be near the statistical 0.5 or even lower (36, 37). Unusually higher 3MP/2MP ratios were first reported by Sachtler *et al.* (38, 39) over Pt/NaY catalysts which were explained in terms of a collimating effect due to the microgeometry of the zeolite. Later, we used similar arguments to explain the high 3MP/2MP ratios observed on the Pt/KL zeolites.

The clear drop in the 3MP/2MP ratio shown in Fig. 3 when the calcination temperature increased from 473 to 773 K indicates that the collimating effect started to disappear as the particles grew outside the zeolite channels.

We can roughly estimate the relative amounts of Pt inside and outside the zeolite channels for the different catalysts by considering that the observed 3MP/2MP ratio is the linear combination of the 3MP/2MP ratios of the Pt sites inside and outside the L zeolite structure, according to the expression

$$(3MP/2MP)_{obs} = s_{in}\,(3MP/2MP)_{in} + s_{out}\,(3MP/2MP)_{out},$$

where s_{in} and s_{out} are the fraction of exposed Pt atoms inside and outside the zeolite channels, respectively. Of course, this relation is only valid if the specific rate of MCP-RO is about the same on sites located inside and outside the zeolite channels. Indeed, Table 1 shows that when the Pt/KL catalyst was calcined at two different temperatures it exhibited a very small variation in TON while the 3MP/2MP ratio significantly varied.

To estimate the fraction of exposed Pt sites inside the zeolite, we assumed that the $(3MP/2MP)_{out}$ ratio for the Pt outside the zeolite was about 0.32. As shown in Table 2, this value was that obtained on the catalyst Pt(out)KL, for which most of the Pt was outside, and it is approximately the same as those obtained on unsupported Pt, and on Pt/SiO_2 catalysts (40, 41). On the other hand, the $(3MP/2MP)_{in}$ ratio can be assumed to be about 1.0–1.2, which are the highest values that we have measured on a large number of samples (12). Based on these values, the estimated fraction of exposed Pt atoms inside the zeolite as a function of calcination temperature has been plotted in Fig. 8. From this estimate, the catalysts precalcined at temperatures below 673 K, have more than 60% of their active area inside the zeolite channels, while after calcination at 773 K, it drops to less than 40%.

An interesting result was obtained for the case of the Pt/BaKL catalyst. First of all, as shown in Table 2, the conversion on this catalyst was significantly lower than that on the catalyst supported on KL zeolite and calcined at the same temperature. However, this decrease did not go together with a similar decrease in the H/Pt ratio, which remained at about the high values typically obtained for Pt/KL catalysts. It would appear that on this Pt/BaL sample, there are Pt sites that are not accessible to MCP, but they are still accessible to hydrogen, resulting in a high H/Pt ratio. In a study of Ba^{2+}- and Sr^{2+}-exchanged L zeolites, Sato

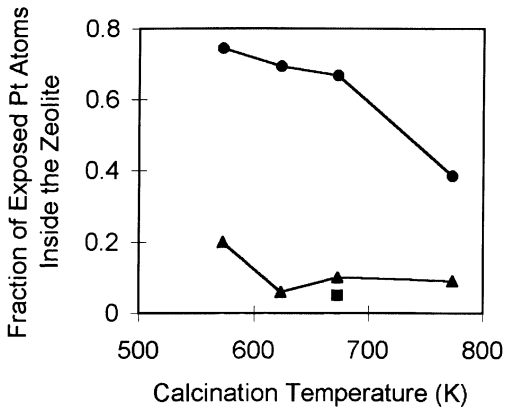

FIG. 8. Fraction of exposed Pt atoms inside the zeolite channels as a function of calcination temperature, estimated from 3MP/2MP ratios obtained on Pt/KL at 613 K (●), Pt/BaKL at 613 K (■), and Pt/BaKL at 603 K (▲).

et al. (42) have recently proposed that, in addition to the normally occupied A, B, C, D, and E exchange sites, some of the M^{2+} ions may occupy exchange sites called F. These sites are located inside the unidimensional channels and if Ba^{2+} ions are anchored there, they would partially block the channels. In that case, they would not allow the access of the bulky MCP molecule, but they would still let the small hydrogen molecule go through and reach the Pt inside the channels. This hypothesis is supported by the analysis done in Fig. 8, which would indicate that, in order to have the observed 3MP/2MP ratio, less than 10% of the exposed Pt atoms should be inside the channels. This estimation would be in contradiction with the relatively high concentration of small particles observed by TEM and the high H/Pt ratio obtained for this catalyst. Therefore, we conclude that a large fraction of the small Pt particles is not accessible to MCP. In agreement with these results, recent studies (43) have proposed that the incorporation of Ba^{2+} into Pt/L catalysts may cause channel blocking.

In summary, the analysis of the 3MP/2MP ratio appears as a very convenient tool to identify preparation and pretreatment conditions that result in significant changes in the location and accessibility of the Pt particles in the L zeolite support. This ratio is higher than the statistical value when collimation effects can be present. Despite the remarkable similarities that Pt/Mg(Al)O and Pt/L catalysts have with respect to aromatization activity, only the Pt/L zeolites exhibit high 3MP/2MP ratios.

The MCP-RO can also be used to study a different phenomenon that takes place during the thermal treatment of the Pt/Mg(Al)O catalysts. In this case, it is the percentage of *n*-hexane in products that carries important information. As mentioned above, only highly coordinatively unsaturated sites can produce *n*-hexane by the MCP-RO. Therefore, the increase in *n*-hexane selectivity as the

reduction temperature increases would indicate an increase in the number of unsaturated Pt sites, particularly considering that this treatment also results in an increase in overall conversion. This is not the typical behavior that one might expect when the reduction temperature increases. Actually, one might expect the opposite, i.e., as the particles become smoother and with a lower degree of coordinative unsaturation, both the activity and selectivity toward *n*-hexane should decrease. This was in fact observed during the second and subsequent cycles. But, what happens during the first cycle? To explain this we have to refer to the "memory effect" displayed by the support, which despite the high calcination temperatures (773 or 873 K) still recuperated the hydrotalcite structure upon exposure to the impregnating solution.

It is conceivable that, during this process, the anionic Pt precursor species ($PtCl_6^{=}$) may become occluded inside the layered structure of the hydrotalcite and the subsequent calcination process is not enough to force the Pt species out of the oxide structure. The reduction following the first calcination step would help the Pt species to come out to the surface. As a result, small metallic particles would start appearing on the surface as the reduction proceeds. This process would explain the high temperature TPR peak as well as the activity and *n*-hexane selectivity variations as a function of reduction temperature during the first cycle. After the first cycle, most of the Pt would be on the surface of the support and subsequent cycles would not change much and behave in a normal way, that is, decreasing activity and *n*-hexane selectivity as the reduction temperature increases. It is interesting to note that in Fig. 7, the more pronounced increase in activity and selectivity occurred for the sample that had been calcined at the lower temperature, 773 K. It seems that during the calcination at 873 K a larger fraction of Pt species were able to come out of the support. Several years ago, we observed similar effects on an apparently very different system. It has been shown that when a highly dispersed Rh/Al_2O_3 catalyst is slowly calcined at high temperatures, Rh species diffused into the bulk of the alumina support. A subsequent reduction causes the metal to come out (44, 45). When we investigated that phenomenon by TPR and MCP-RO (46) the observed behavior was almost the same as that displayed by the Pt/Mg(Al)O catalysts; that is, the activity and *n*-hexane selectivity increased during the first cycle as the Rh species appeared on the surface. Subsequent cycles, resulted in a slight sintering preventing further diffusion into the bulk, and in consequence, both the activity and selectivity decrease with increasing reduction temperatures, as expected.

CONCLUSIONS

The analysis of the product distribution of the methylcyclopentane ring opening reaction is an effective technique to study morphological changes in Pt catalysts supported on non-acidic materials. We have used it in combination with electron microscopy (TEM), temperature programmed reduction (TPR), and hydrogen chemisorption to investigate a series of catalysts of Pt/L zeolites and Pt/Mg(Al)O. In particular, two parameters in the product distribution carry important information:

(a) the 3MP/2MP ratio is a good indicator of the presence of collimation effects. In the case of the Pt/L zeolite catalysts, we have used it to determine the location of the Pt particles and detect channel blocking. Accordingly, we determined that a high temperature calcination treatment resulted in a migration of the Pt species out of the zeolite channels and that the presence of Ba^{2+} ions may result in a partial blocking of the zeolite channels.

(b) the percentage of *n*-hexane in products is an indicator of the presence of coordinatively unsaturated sites. Through the analysis of this parameter during oxidation–reduction cycles on Pt/Mg(Al)O catalysts, we postulated that a large fraction of Pt species become trapped inside the bulk of the support and only come out to the surface after a cycle of oxidation/reduction at relatively high temperatures.

ACKNOWLEDGMENTS

We thank the University of Mar del Plata for a fellowship for one of us (W.E.A.), as part of the international exchange program sponsored by the University of Oklahoma and the University of Mar del Plata. Partial support from NSF-CONICET International Program (INT-9415590) is acknowledged. We thank Mr. Jorge Cechini for his assistance in the preparation of the Mg(Al)O support, and Professor C. E. Gigola (Plapiqui, UNS) for letting us use their TPR facilities.

REFERENCES

1. Bai, X., and Sachtler, W. M. H., *J. Catal.* **132**, 165 (1991).
2. Bai, X., Zhang, Z., and Sachtler, W. M. H., *Appl. Catal.* **72**, 165 (1991).
3. Lerner, B. A., Corbvill, B. T., and Sachtler, W. M. H., *Catal. Lett.* **18**, 227 (1993).
4. Sachtler, W. M. H., and van Santen, R. A., *Adv. Catal.* **26**, 69 (1977).
5. van Senden, F. G., van Broekhoven, E. H., Wreesman, C. T. J., and Ponec, V., *J. Catal.* **87**, 468 (1985).
6. O'Cinneide, A., and Gault, F. G., *J. Catal.* **37**, 311 (1975).
7. Dees, M. J., Bol, M. H. B., and Ponec, V., *Appl. Catal.* **64**, 279 (1990).
8. Schepers, F. J., van Senden, J. G., van Broekhoven, E. H., and Ponec, V., *J. Catal.* **94**, 400 (1985).
9. Resasco, D. E., and Haller, G. L., *J. Catal.* **82**, 279 (1983).
10. Fenoglio, R. J., Nuñez, G. M., and Resasco, D. E., *J. Catal.* **120**, 1 (1989).
11. Gault, F. G., *Adv. Catal.* **30**, 7 (1981).
12. Alvarez, W. E., and Resasco, D. E., *Catal. Lett.* **8**, 53 (1991).
13. Moretti, G., and Sachtler, W. M. H., *J. Catal.* **116**, 361 (1989).
14. McVicker, G. B., Kao, J. L., Ziemiak, J. J., Gates, W. E., Robins, J. L., Treacy, M. M. J., Rice, S. B., Vanderspurt, T. H., Cross, V. R., and Ghosh, A. K., *J. Catal.* **139**, 48 (1993).
15. Fukunaga, T., and Ponec, V., *J. Catal.* **157**, 550 (1995).
16. Reagan, W. J., Chester, A. W., and Kerr, G. T., *J. Catal.* **69**, 89 (1981).
17. Ostgard, D. J., Kustov, L., Poeppelmeier, L., and Sachtler, W. M. H., *J. Catal.* **133**, 342 (1992).

18. Larsen, G., Ph.D. thesis, Yale University, p. 33, 1994.
19. Davis, R. J., and Mielczarski, E., *in* "Selectivity in Catalysis" (M. E. Davis and S. L. Suib, Eds.), Ch. 22, p. 327. American Chemical Society, 1993.
20. Schaper, H., Berg-Slot, J. J., and Stork, W. H. J., *Appl. Catal.* **54**, 79 (1989).
21. Cavani, F., Trifirio, F., and Vaccari, A., *Catal. Today* **11**, 173 (1991).
22. Labajos, F. M., Rives, V., and Ulibarri, M. A., *J. Mater. Sci.* **27**, 1546 (1992).
23. Valcheva-Traykova, M. L., Davidova, N. P., and Weiss, A. H., *J. Mater. Sci.* **28**, 2157 (1993).
24. Bernard, J. R., *in* "Proc. 5th Int. Zeolite Conf." (L. V. Rees, Ed.), p. 686. Heyden, London, 1980.
25. Hughes, T. R., Buss, W. R., Tamm, P. W., and Jacobson, R. L., *Stud. Surf. Sci. Catal.* **28**, 725 (1986).
26. Davis, R. J., and Derouane, E. G., *Nature (London)* **349**, 313 (1991).
27. Davis, R. J., and Derouane, E. G., *J. Catal.* **132**, 269 (1991).
28. Besoukhanova, C., Guidot, J., Barthomeuf, D., Breysse, M., and Bernard, J. R., *J. Chem. Soc. Faraday Trans. 1* **77**, 1595 (1981).
29. Larsen, G., and Haller, G. L., *Catal. Lett.* **3**, 103 (1989).
30. Larsen, G., McHugh, B. J., and Haller, G. L., *J. Phys. Chem.* **94**, 8621 (1990).
31. Kazansky, V. B., Borokov, V. Y., and Derouane, E. G., *Catal. Lett.* **19**, 331 (1993).
32. Tauster, S. J., and Steger, J. J., *J. Catal.* **125**, 387 (1990).
33. Iglesia, E., and Bumgartner, J. E., *in* "New Frontiers in Catlaysis" (L. Guczi, F. Solymosi, and P. Tetenyi, Eds.), Vol. 75B, p. 993. Studies in Surface Science and Catalysis, Elsevier, Amsterdam, 1993.
34. Davis, R. J., HCR Concise Review, p. 41. Wiley, New York, 1994.
35. Mileczarski, E., Hong, S. B., Davis, R. J., and Davis, M. E., *J. Catal.* **134**, 359 (1992).
36. Gault, F. G., Garin, F., and Maire, G., *in* "Growth and Properties of Metal Clusters" (J. Bourdon, Ed.), p. 451. Elsevier, Amsterdam, 1980.
37. van Senden, J. G., van Broekhoven, E. H., Wreesman, C. T. J., and Ponec, V., *J. Catal.* **87**, 468 (1985).
38. Chow, M., Park, S. H., and Sachtler, W. M. H., *Appl. Catal.* **19**, 349 (1985).
39. Moretti, G., and Sachtler, W. M. H., *J. Catal.* **115**, 205 (1989).
40. Anderson, J. R., and Shimoyama, Y., *in* "Proc. V International Congress on Catalysis, Palm Beach, 1972" (J. W. Hightower, Ed.), p. 895. North-Holland, Amsterdam, 1973.
41. Kramer, R., and Zueg, H., *J. Catal.* **85**, 530 (1984).
42. Sato, M., Morikawa, K., and Kurosawa, S., *Eur. J. Mineral.* **2**, 851 (1990).
43. Gao, Z., Jiang, X., Ruan, Z., and Xu, Y., *Catal. Lett.* **19**, 81 (1993).
44. Wong, C., and McCabe, R., *J. Catal.* **119**, 47 (1989).
45. Wong, C., and McCabe, R., *J. Catal.* **101**, 123 (1986).
46. Alvarez, W. E., Fenoglio, R. J., Nuñez, G. M., and Resasco, D. E., *in* "Catalysis Deactivation 1991" (C. H. Bartholomew, Ed.), p. 613. Elsevier, Amsterdam, 1991.